Journal of Asian Concrete Federation
Vol. 11, No. 3, pp. 35-48, September 2025
ISSN 2465-7964/ eISSN 2465-7972
DOI http://dx.doi.org/10.18702/acf.2025.11.3.35

Technical Paper

Preparation of ultra–high strength concrete for CFST arches

Li Li, Fangmei Huang *, Baochun Chen

(Received: 17-Aug-2025; Revised: 23-Sep-2025; Accepted: 24-Sep-2025; Published online: 30-Sep-2025)

Abstract: The application of ultra-high strength concrete (UHSC) in concrete-filled steel tube (CFST) arches significantly enhances the structural load-bearing capacities. However, to meet the pumping construction requirement and ensure a composite effect between the steel tube and core concrete without debonding, core UHSC should simultaneously achieve ultra-high compressive strength, high flowability, and low shrinkage or micro expansion characteristics. In this paper, the preparation technology for such UHSC is systematically studied. The effects of coarse aggregate, steel fiber, expansion agent, and shrinkage-reducing agent on the compressive strength, flowability, and autogenous shrinkage of UHSC are investigated. The results indicate that UHSC with an appropriate amount of coarse aggregates (0~41.6% replacement ratio by mass) or steel fibers (0~2% by volume) satisfied the target compressive strength and flowability, while the risk of debonding still existed due to the shrinkage of the core UHSC. Optimal performance to prevent debonding was achieved through the combined use of coarse aggregates (21.6%) with hybrid admixtures (10% expansion agent + 1~2% shrinkage reducing agent). A mixed design approach for the core UHSC filled into the CFST arch is finally proposed.

Keywords: Ultra-high strength concrete; CFST arch; Coarse aggregate; Steel fiber; Expansion agent; Shrinkage-reducing agent

1.Introduction

The application of ultra-high strength concrete (UHSC) in concrete filled steel tube (CFST) arches significantly enhances the structural load-bearing capacities, demonstrating broad application prospects in large span and ultra-large span CFST arch bridges, as well as Melan arch bridges employing CFST arches as embedded frameworks [1-3]. To meet the pumping construction requirement and ensure composite effect between steel tube and core concrete without debonding, core UHSC should simultaneously achieve ultra-high compressive strength, high flowability, and low shrinkage or micro expansion characteristics [4]. According to the Chinese reactive powder concrete standard (GB/T 31387-2015 [5]), concrete with a cubic compressive strength greater than or equal to 100 MPa is categorized as UHSC. According to the Chinese technical code for CFST arch bridges (GB/T 50923-2013 [6] and JTG/T D65-06-2015 [7]), the minimum slump flow of core UHSC tested using the standard slump cone should be 500 mm. Additionally, the critical autogenous shrinkage of UHSC should be less than 100 με to ensure the shrinkage-induced stress is smaller than steel-concrete interfacial bond strength [8].

The preparation technology for core UHSC that meets the requirements for compressive strength, flowability, and autogenous shrinkage has not yet been fully studied. To reduce the autogenous shrinkage of UHSC, an approach is to add coarse aggregates in the mix [9-12]. However, the interfacial transition zones (ITZ) between coarse aggregate and paste matrix may negatively impact the concrete compressive strength.

*Corresponding author **Fangmei Huang,** *School of Civil Engineering, Fujian University of Technology, Fujian 350000, China. E–mail: fangmeihuang@fjut.edu.cn*
Li Li, *College of Civil Engineering, Fuzhou University, Fujian 350000, China. E–mail: 877150982@qq.com*
Baochun Chen, *College of Civil Engineering, Fuzhou University, Fujian 350000, China;School of Civil Engineering, Fujian University of Technology, Fujian 350000, China. E–mail: 584601514@qq.com*

Moreover, coarse aggregates harm the uniform dispersion of steel fibers in the matrix, leading to fiber clustering and a significant reduction in the flowability of UHSC [11]. Steel fibers, characterized by high tensile strength and elastic modulus, are widely utilized in UHSC to enhance the mechanical properties and mitigate the autogenous shrinkage [13-15]. However, the addition of steel fibers leads to reduced flowability of UHSC. In practical engineering, the commonly used dosage of steel fibers is 2%~3% by volume to balance these factors and cost [16]. Expansion agent (EA) is commonly used to compensate for the autogenous shrinkage of UHSC, but usually results in a reduction in both compressive strength and flowability [17-18]. It is noted that UHSC is characterized by a low water-to-binder ratio (*w/b*), resulting in insufficient water for EA to achieve full expansion potential. Moreover, UHSC may experience expansion rebound when EA is used individually [19]. Therefore, the combined use of EA and shrinkage-reducing agent (SRA) has been investigated to achieve synergistic effects [20-21].

To prepare core UHSC equipped with ultra-high compressive strength ($f_{cu,100} \geq 100$ MPa), high flowability (slump flow ≥ 500 mm), and low shrinkage or micro expansion (autogenous shrinkage ≤ 100 με), a systematical experiment program is carried out to investigate the effects of coarse aggregate, steel fiber, EA and SRA on the compressive strength, flowability and autogenous shrinkage of UHSC. The research aims to provide technical support for UHSC applications in CFST arches.

2. Experimental program

2.1 Materials

The raw materials in this study included P·O 42.5 ordinary portland cement, silica fume (SiO_2 content ≥ 90%, specific surface area:18.92 m^2/g), fly ash (specific surface area: 0.6 m^2/g), quartz sand (particle size: 0.075 mm ~ 2.0 mm), granite coarse aggregate (particle size: 4.75 mm ~ 9.5 mm), CX-8 polycarboxylate superplasticizer (water reducing rate: 25%), HME®-II high performance expansion agent, SBT®-SRA polyether-based shrinkage reducing agent, straight steel fiber (length: 13 mm, diameter: 0.2 mm, tensile strength ≥ 2200 MPa), tap water.

2.2 Mix proportions

As shown in Table 1, the mix proportions in this study were adjusted from the reference mixture used in our previous studies [11,22], with the original cementitious material content (1118 kg/m^3), superplasticizer content (21.5 kg/m^3), and water-to-binder ratio (0.16) being maintained. The aggregate gradation (quartz sand and coarse aggregate) was optimized using the Modified Andreasen and Andersen (MAA) particle packing model [23], which yielded two design mixtures: CA0 (without coarse aggregate) and CA31.6 (coarse aggregate replacement ratio of 31.6%).

The nomenclature of mixtures in this table indicates the coarse aggregate replacement ratio (e.g., "CA31.6" means the coarse aggregate replacement ratio is 31.6%), steel fiber volume content (e.g., "SF1" means the steel fiber volume content is 1%), EA dosage (e.g., "E8" means the EA dosage is 8%), and SRA dosage (e.g., "R0.5" means the SRA dosage is 0.5%). It is noted that coarse aggregate was incorporated by equivalently replacing quartz sand, EA was incorporated by equivalently replacing cementitious materials [21,24], while SRA dosage was calculated as a percentage of cementitious materials [21].

Furthermore, these mixtures were categorized into five groups depending on the variables. Group I examined the coarse aggregate replacement ratio using five mixtures: the two MAA-optimized reference mixtures CA0 and CA31.6, and three additional mixtures adjusted from CA31.6. Group II consisted of four mix proportions with steel fiber volume content as the variable, using CA0 and CA21.6 from Group I as reference control mixtures. Group III and Group IV each consisted of three mix proportions with EA dosage and SRA dosage as their respective variable, and CA21.6 was used as the reference control mixture. Group V consisted of four mix proportions, where EA and SRA were used in combination.

2.3 Samples preparation

For each batch of UHSC, six cubes of 100 mm × 100 mm × 100 mm for compressive strength testing

were cast in concrete molds, and two cylinders of φ100 mm × 515 mm for autogenous shrinkage measurement were cast in polyvinyl chloride(PVC) tubes (internal diameter: 100 mm, length: 515 mm). All specimens were immediately covered with a plastic sheet to prevent moisture loss. The UHSC cubes were demolded 24 hours after casting and subsequently cured under natural conditions (average ambient temperature: 19.5 ℃ at daytime and 11.3 ℃ at night) with continuous plastic film wrapping until the test age (28 d). The UHSC cylinders were moved to the laboratory without demolding. The temperature in the laboratory was maintained at 20 ± 2 ℃ .

2.4 Test methods

The compressive cubic strength of UHSC was tested according to the Chinese reactive powder concrete standard (GB/T 31387-2015 [6]). A 2000 kN universal testing machine was employed, and the loading rate was set as 1.2 MPa/s, see Fig. 1(a). At least three cubes of 100 mm × 100 mm × 100 mm for each UHSC batch were tested to further calculate the average strength.

The slump flow of UHSC was measured by using a standard slump cone (top diameter: 100 mm, bottom diameter: 200 mm, height: 300 mm) according to the Chinese standard for test method of performance on ordinary fresh concrete (GB/T 50080-2016 [25]), see Fig.1(b). Fresh UHSC was cast in the cone by three layers, and each layer was compacted with 25 strokes using a tamping rod. Afterwards, the cone was lifted vertically within 3s ~ 6s to allow the paste to flow freely without vibrating. The slump flow was recorded as the average value of two perpendicular measurements.

The autogenous shrinkage of UHSC was measured per Chinese standard for test methods of long-term performance and durability of ordinary concrete (GB/T 50082-2009 [26]), as shown in Fig. 1(c). The PVC tubes were placed in the vertical shrinkage frames after casting. The final setting time was marked as a start point for the autogenous shrinkage [27-29]. The exposed surface of core UHSC was wrapped with plastic film until final setting, followed by a uniform paraffin wax coating to prevent moisture exchange. The deformations of two specimens were tested for each mixture to further calculate the average autogenous

Table 1 Mix proportions of UHSC (kg/m^3)

Group	Mixtures	Cement	Silica fume	Fly ash	Coarse aggregate (4.75~9.5 mm)	Quartz sand				Steel fiber	EA	SRA
						0.85~2.0 mm	0.425~0.85 mm	0.212~0.425 mm	0.075~0.425 mm			
I	CA0	860	129	129	0	339.0	229.4	197.2	240.4	0	0	0
	CA11.6	860	129	129	116.7	384.6	168.5	148.2	187.9	0	0	0
	CA21.6	860	129	129	217.3	341.1	149.5	131.5	166.6	0	0	0
	CA31.6	860	129	129	317.4	297.8	130.5	114.8	145.5	0	0	0
	CA41.6	860	129	129	418.6	254.1	111.3	97.9	124.1	0	0	0
II	CA0SF1	860	129	129	0	339.0	229.4	197.2	240.4	78.5	0	0
	CA0SF2	860	129	129	0	339.0	229.4	197.2	240.4	157.0	0	0
	CA21.6SF1	860	129	129	217.3	341.1	149.5	131.5	166.6	78.5	0	0
	CA21.6SF2	860	129	129	217.3	341.1	149.5	131.5	166.6	157.0	0	0
III	CA21.6E6	808.4	121.3	121.3	217.3	341.1	149.5	131.5	166.6	0	67.1	0
	CA21.6E8	791.2	118.7	118.7	217.3	341.1	149.5	131.5	166.6	0	89.4	0
	CA21.6E10	774.0	116.1	116.1	217.3	341.1	149.5	131.5	166.6	0	111.8	0
IV	CA21.6R0.5	860	129	129	217.3	341.1	149.5	131.5	166.6	0	0	5.6
	CA21.6R1.0	860	129	129	217.3	341.1	149.5	131.5	166.6	0	0	11.2
	CA21.6R2.0	860	129	129	217.3	341.1	149.5	131.5	166.6	0	0	22.4
V	CA21.6E8R1.0	791.2	118.7	118.7	217.3	341.1	149.5	131.5	166.6	0	89.4	11.2
	CA21.6E8R2.0	791.2	118.7	118.7	217.3	341.1	149.5	131.5	166.6	0	89.4	22.4
	CA21.6E10R1.0	774.0	116.1	116.1	217.3	341.1	149.5	131.5	166.6	0	111.8	11.2
	CA21.6E10R2.0	774.0	116.1	116.1	217.3	341.1	149.5	131.5	166.6	0	111.8	22.4

shrinkage.

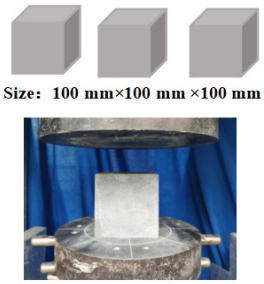

(a)Compressive test

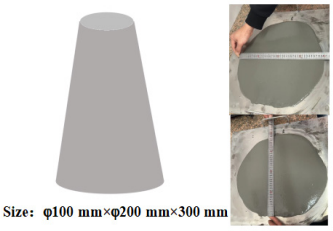

(b)Flowability test

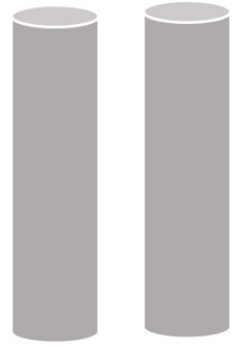

(c)Autogenous shrinkage test

Fig. 1 Performance test projects of UHSCResults and discussion

3.1 Compressive strength

Fig.2(a) illustrates the effect of coarse aggregate replacement ratio on the 28-day cubic compressive strength ($fcu,100$) of UHSC. The test results demonstrate that, in contrast to the coarse aggregate-free mixture CA0, the compressive strengths of mixtures containing coarse aggregate exhibited a non-monotonic dependence on coarse aggregate replacement ratio. Specifically, CA11.6 and CA41.6 showed reductions of 1.7% and 5.3% respectively, while CA21.6 and CA31.6 exhibited enhancements of 7.1% (peak) and 4.0% respectively. This implies that UHSC containing coarse aggregates could achieve comparable or even enhanced compressive strength when the aggregate gradation is appropriately designed, which aligns with Ref [11, 30, 31].

This finding can be explained by previous research on the microstructure of UHSC containing coarse aggregates. The compressive strength of concrete depends on the paste matrix, aggregate, and the ITZ between them. For UHSC, the ITZ between paste matrix and coarse aggregate could be significantly enhanced due to the formation of a large amount of calcium silicate hydrate (C-S-H, a key pozzolanic reaction product and major contributor to concrete strength) [32,33], and the micro aggregate effect of mineral admixtures [9,32-36], which eliminates ITZ as the traditional weakest link in the concrete. Additionally, the cracks may propagate directly through the coarse aggregate due to the obviously enhanced paste matrix and ITZ in UHSC, allowing the inherent strength of coarse aggregate to be fully utilized [32]. Therefore, appropriate type and content of coarse aggregates present a positive effect on the compressive strength of UHSC [9].

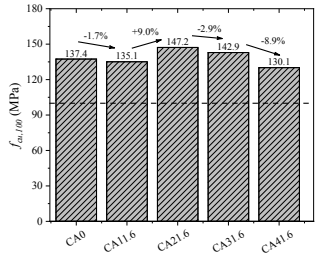

(a)Coarse aggregate replacement ratio

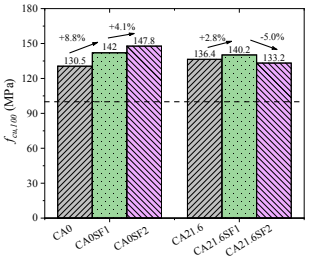

(b)Steel fiber volume content

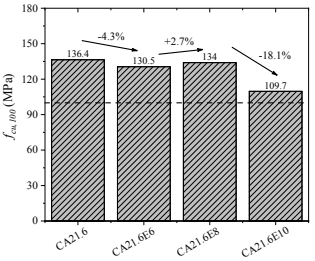

(c)EA dosage

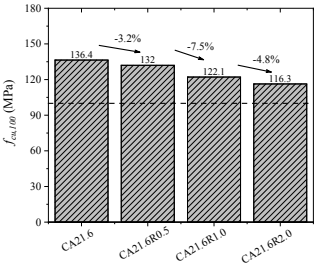

(d)SRA dosage

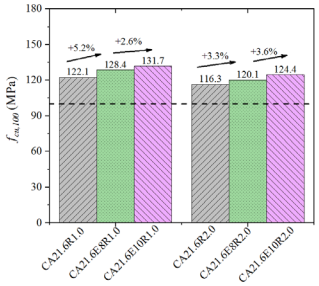

(e)Combined dosage of EA and SRA

Fig. 2 Compressive strength of UHSC

Fig.2(b) illustrates the cubic compressive strength of UHSC incorporating various steel fiber volume content (0%, 1% and 2%). Since the adjusted mixture CA21.6 achieved higher compressive strength than the MAA model-calculated mixture CA31.6, it was selected as the reference mixture to investigate the combined effect of coarse aggregates and steel fibers on UHSC properties. For coarse aggregate-free UHSC, the compressive strength was enhanced by 8.8% when steel fiber volume content increased from 0% to 1%, and exhibited a cumulative enhancement of 13.2% when steel fiber volume content was increased to 2%. In contrast, for UHSC containing coarse aggregates, the addition of 1% steel fibers improved the compressive strength by 2.8%, while the addition of 2% steel fibers resulted in a 2.3% reduction in compressive strength.

This contrasting behavior can be explained by the underlying mechanisms identified in previous studies. The addition of steel fibers delays the formation and propagation of cracks, thereby increasing the compressive strength of UHSC [37,38]. However, the inclusion of coarse aggregates decreases the fiber dispersion coefficient and orientation coefficient, which diminishes the crack-bridging efficiency of steel fibers and consequently exerts a negative impact on the compressive strength of UHSC [33,39,40]. It should be noted that the coarse aggregates and steel fibers used in this study are not matched since the maximum particle size of the coarse aggregates (9.5 mm) exceeds 2/3 of the fiber length (13 mm) [41]. Moreover, the degree of mismatch increases with steel fiber volume content [39]. As a result, the compressive strength of UHSC containing coarse aggregates exhibited fluctuating variations with increasing steel fiber volume content.

Fig. 2(c) illustrates the effect of EA dosage on the compressive strength of UHSC. The test results revealed that, in comparison to EA-free mixture CA21.6, mixtures incorporating EA exhibited strength reductions, with 4.3%, 1.8% and 19.9% at EA dosages of 6%, 8%, and 10% respectively. This finding is consistent with Ref [18,19,42-44]. Previous studies have demonstrated that the incorporation of EA exerts both beneficial and adverse effects on the compressive strength of UHSC. On the positive side, the expansion products of EA can effectively mitigate the shrinkage of UHSC during the hardening process, thereby minimizing micro-crack formation [45]. Additionally, these expansion products refine the microstructure of UHSC due to the filling effect [46-50]. However, there are mainly five factors contributing to the compressive loss of UHSC incorporating EA: (i) the partial replacement of cement by EA reduces the cement content [43,46,50] since the expansion products of EA contribute less to the strength development as compared to cement hydration products [18,44,51,52]; (ii) the water competition between EA and cement impairs the hydration reaction [44,53]; (iii) the expansion products cover the cement surface, forming a layer of dense gel that blocks water entry and hinders further cement hydration [54,55]; (iv) the internal pressure generated when EA hydration products fill pores may induce crack formation [21,46,50,56,57]; (v) the quality of ITZ between the hardening cement paste and the hydration products of EA tends to be decreased [46,58]. Therefore, the compressive strength of UHSC exhibited a non-monotonic decreasing trend with the increase in EA dosage.

Fig. 2(d) illustrates the effect of SRA dosage on the compressive strength of UHSC. The test results showed that, compared with the SRA-free mixture CA21.6, mixtures incorporating SRA exhibited strength reductions of 3.2%, 10.5%, and 14.7% at SRA dosages of 0.5%, 1.0%, and 2.0%, respectively. This is consistent with previous studies [29,59-66]. The strength reduction is primarily attributed to the decreased cement hydration degree and pozzolanic reaction of mineral admixtures, as reflected by increased porosity[29,66-68] and diminished ITZ quality [58]. Specifically, the incorporation of SRA increases the pH value of the pore solution, leading to a decrease in alkali concentration and limiting the dissolution of C3A, thereby reducing the formation of hydration products [66]. Moreover, the adsorption of SRA on the surface of raw materials and hydration products decelerates the development of microstructure to a great extent [63,65,66].

Fig. 2(e) compares the compressive strength of UHSC with different combinations of EA and SRA. The test results demonstrated that, at a fixed SRA content, the compressive strength increased with EA dosage. Specifically, when the SRA dosage was 1%, the compressive strengths of CA21.6E8R1.0 (8%

EA+1.0% SRA) and CA21.6E10R1.0 (10% EA+1.0% SRA) were increased by 5.2% and 7.9% respectively, as compared to the reference mixture CA21.6R1.0 (1.0% SRA). When the SRA dosage was 2%, the compressive strengths of CA21.6E8R2.0 (8% EA+2.0% SRA) and CA21.6E10R2.0 (10% EA+2.0% SRA) were increased by 3.3% and 7.0% respectively, as compared to the reference mixture CA21.6R2.0 (2.0% SRA). This indicates that the combined use of EA and SRA can compensate for the negative effect of SRA on the compressive strength of concrete. Similar conclusions have been drawn in Ref [21,69-71].

It is noted that the black dashed lines in Fig. 2 represent the compressive strength threshold of core UHSC ($f_{cu,100} = 100MPa$). It can be seen that all mixtures listed in Table 1 satisfied the minimum compressive strength requirement.

3.2 Flowability

Fig. 3(a) illustrates the slump flow of fresh UHSC with varying coarse aggregate replacement ratios (0~41.6%). The test results revealed that, despite the identical w/b ratio and superplasticizer dosage, the flowability of UHSC increased first and then decreased as the coarse aggregate replacement ratio increased. This phenomenon can be primarily attributed to the fact that the specific surface area of coarse aggregate is smaller than that of fine aggregate, leading to a reduction in slurry required to coat the aggregates and thus enhancing the flowability [72-74]. However, when the coarse aggregate replacement ratio was increased to 41.6%, the packing density tended to decrease. Consequently, more slurry was consumed as a lubricant between aggregates, and the interlocking effect between the coarse aggregates hindered the flow of fresh UHSC [75].

Fig. 3(b) illustrates the effect of steel fiber volume content on the slump flow of UHSC. A general flowability decrease was observed with increasing steel fiber volume content, particularly for UHSC containing coarse aggregates. For example, mixture CA21.6 exhibited a 13.1% higher slump flow than mixture CA0 when no steel fibers were added, while mixture CA21.6SF2 exhibited an 8.5% lower slump flow than mixture CA0SF2 when 2% steel fibers were added. Similar observations have been reported in Ref [76-77]. The flowability reduction of UHSC incorporating steel fibers is mainly due to the friction and interlocking between the fiber, paste, and aggregate [78-79]. The incorporation of coarse aggregates leads to a more severe interlocking effect of steel fibers, and thus fibers entangle and form larger clumps or balls, resulting in further reduction in flowability [76].

Fig. 3(c) shows the effect of EA dosage on the slump flow of fresh UHSC. It is observed that as the EA dosage increased from 0% to 6%, 8%, and 10%, the slump flow of UHSC was reduced by 12.4%, 18.7%, and 29.2%, respectively. This trend is consistent with previous studies, i.e., the flowability of UHSC decreases with increasing EA dosage [18,45,49,50]. This is mainly because EA consumes water to form a water film, leading to water competition with cement and thereby significantly reducing the available free water in fresh UHSC [18,44,80]. Moreover, the specific surface area of EA is larger than that of cement, which needs more water to achieve saturation and form a water film [81-83].

Fig. 3(d) presents the effect of SRA dosage on the slump flow of fresh UHSC. The test results demonstrated that the flowability of UHSC increased with SRA dosage. Specifically, when the SRA dosage was increased from 0% to 0.5%, 1.0%, and 2.0%, the slump flow of UHSC was increased by 5.9%, 7.9%, and 10.1%. Similar findings have been reported in Ref [24,29,60]. This is mainly because the synergistic effect between SRA and polycarboxylate superplasticizer enhances the initial fluidity of paste [24,83]. Moreover, the water contained in SRA increases the w/b of UHSC [29,60,84].

Fig. 3(e) illustrates the slump flow of fresh UHSC incorporating different combinations of EA and SRA. The test results demonstrated that at a constant EA dosage, the flowability of UHSC increased with SRA dosage. Specifically, when the EA dosage was 8%, the slump flow of CA21.6E8R1.0 (8% EA+1.0% SRA) and CA21.6E8R2.0 (8% EA+2.0% SRA) were increased by 10.7% and 17.9% respectively, as compared to the reference mixture CA21.6E8 (8% EA). When the EA dosage was 10%, the slump flow of CA21.6E10R1.0 (10% EA+1.0% SRA) and CA21.6E10R2.0 (10% EA+2.0% SRA) were increased by 17.8% and 22.8%

respectively, as compared to the reference mixture CA21.6E10 (10% EA). This indicates that the combined use of EA and SRA can compensate for the negative effect of EA on the flowability of concrete.

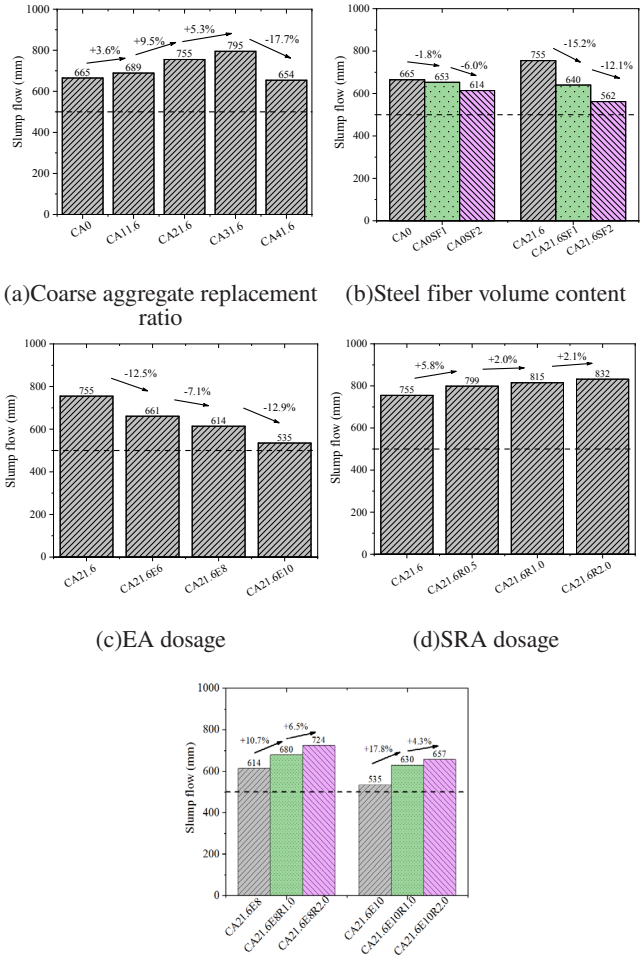

(a)Coarse aggregate replacement ratio

(b)Steel fiber volume content

(c)EA dosage

(d)SRA dosage

(e)Combined dosage of EA and SRA

Fig. 3 Slump flow of UHSC

The black dashed lines in Fig. 3 represent the threshold of slump flow for core UHSC (Slump flow = 500 mm). Overall, each mixture listed in Table 1 satisfies the minimum slump flow requirement. It is noted that the mixtures CA21.6SF2 (21.6% coarse aggregates and 2% steel fibers) and CA21.6E10 (21.6% coarse aggregates and 10% EA) both exhibited marginal flowability with slump flows of merely 562 mm and 535 mm, respectively. Therefore, further increases in steel fiber volume content and EA dosage would be impractical for maintaining adequate flow performance when the coarse aggregate content is fixed (21.6%).

3.3 Autogenous shrinkage

The autogenous shrinkage of UHSC mixtures listed in Table 1 is illustrated in Fig. 4 with age as the horizontal coordinate. Negative values in this figure denote expansion behavior, and the black dashed lines represent the threshold of autogenous shrinkage for core UHSC (100 με). Overall, the test results revealed that the autogenous shrinkage process can be categorized into three stages: early stage (0~7 d), intermediate stage (7~28 d), and late stage (>28 d) [11]. At an early age, the autogenous shrinkage develops rapidly due to the high hydration rate and low elasticity modulus at this stage [11,85,86], accounting for over 75% of the total autogenous shrinkage. At the intermediate stage, the development of autogenous shrinkage decelerates, followed by stabilization at the late stage. Therefore, the 90-day autogenous shrinkage serves as the criterion for assessing compliance with the requirement of core UHSC.

It can be seen in Fig. 4(a) that the incorporation of 11.6%, 21.6%, 31.6% and 41.6% coarse aggregates decreased the 90-day autogenous shrinkage by 9.5%, 16.3%, 20.2% and 21.5% respectively. This mitigation effect stems from the fact that the high-strength coarse aggregates form an equivalent skeleton structure acting as a fixed-volume component [75], leading to enhancement in the volume stability and thereby restraining the autogenous shrinkage of the surrounding cement paste. Nevertheless, the autogenous shrinkage values of mixtures incorporating 11.6%~41.6% coarse aggregates remained substantial (487~541με), exceeding the target threshold (100 με) and thereby maintaining a potential interfacial debonding risk between core UHSC and steel tube.

As shown in Fig. 4(b), the addition of steel fibers is effective in restraining the autogenous shrinkage of UHSC. Specifically, when the steel fiber volume content increased from 0% to 1%, the 90-day autogenous shrinkage values of UHSC were reduced by 30.1% (without coarse aggregates) and 27.5% (with coarse aggregates). However, when the steel fiber volume content further increased from 1% to 2%, the shrinkage-reducing effect of steel fibers became less pronounced, with additional reductions of only 9.0% and 8.4% for UHSC without and with coarse

aggregates, respectively. This is consistent with the observations from Ref [15]. The restraining mechanism is mainly because the high-stiffness steel fibers can effectively resist the capillary tensions by preventing the matrix movement [14-15]. Moreover, steel fibers can decrease the presence of pores larger than 50 nm, which also contributes to reducing autogenous shrinkage [87].

Additionally, at a fixed steel fiber volume content, UHSC mixtures with coarse aggregates demonstrated lower autogenous shrinkage values than their counterparts without coarse aggregates. Specifically, CA0SF1 exhibited a 9.1% higher autogenous shrinkage than CA21.6SF1, while CA0SF2 exhibited a 7.5% higher autogenous shrinkage than CA21.6SF2. This phenomenon indicates a synergistic effect of coarse aggregate and steel fiber in mitigating autogenous shrinkage. Notably, UHSC mixtures reinforced with steel fibers (Group II in Table 1) still exhibited a considerably high autogenous shrinkage, with the minimum autogenous shrinkage (445 με) significantly exceeding the autogenous shrinkage threshold of core UHSC (100 με).

As illustrated in Fig. 4(c), the autogenous shrinkage of UHSC was significantly reduced by the incorporation of EA. When the EA dosage increased from 0% to 6%, 8%, and 10%, the 90-day autogenous shrinkage values of UHSC were reduced by 42.2%, 63.0%, and 66.9%, respectively. Notably, although a micro-expansion phenomenon at 1 d was observed for UHSC with 10% EA (CA21.6E10), its 90 d autogenous shrinkage still reached 185 με, exceeding the target threshold of 100 με. The limited effectiveness of EA at high dosage can be attributed to the low water-to-binder ratio characteristic of UHSC, where early cement hydration consumes a large amount of water, leaving insufficient moisture for EA to react and form stable hydrate products [19].

As shown in Fig. 4(d), the incorporation of SRA can significantly reduce the autogenous shrinkage of UHSC. Compared with mixture CA21.6, the counterpart mixtures exhibited 90-day autogenous shrinkage reductions of 22.4%, 38.8%, and 51.7% at SRA dosages of 0.5%, 1.0%, and 2.0%, respectively. This reduction is mainly due to the beneficial effect of SRA on decreasing the surface tension of the pore solution [63,67]. It should be pointed out that the mixture with 2% SRA (CA21.6R2.0) still exhibited a 90-day autogenous shrinkage of 263 με, exceeding the target threshold of 100 me.

It can be concluded from Fig. 4(e) that the combined use of EA and SRA has a synergistic effect in preparing low-shrinkage or micro expansion UHSC. Similar findings have been reported in Ref [20,21,46,58]. Notably, mixtures CA21.6E10R1.0 (21.6% coarse aggregates, 10% EA, and 1.0% SRA) and CA21.6E10R2.0 (21.6% coarse aggregates, 10% EA, and 2.0% SRA) exhibited significantly reduced autogenous shrinkage values of 83 με and 32 με respectively, below the target threshold of 100 me.

To sum up, the optimized mixtures CA21.6E10R1.0 (21.6% coarse aggregates, 10% EA, and 1.0% SRA) and CA21.6E10R2.0 (21.6% coarse aggregates, 10% EA, and 2.0% SRA) could simultaneously fulfill all criteria for the compressive strength, flowability, and debonding resistance of core UHSC.

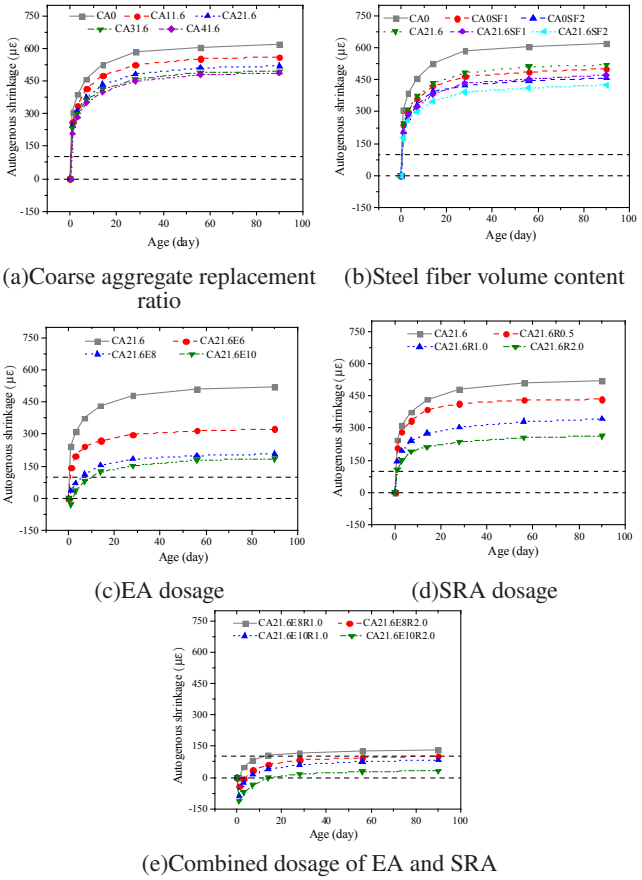

(a)Coarse aggregate replacement ratio (b)Steel fiber volume content

(c)EA dosage (d)SRA dosage

(e)Combined dosage of EA and SRA

Fig. 4 Autogenous shrinkage of UHSC

Conclusions

In this study, the mix proportions of core UHSC that are equipped with ultra-high compressive strength (fcu,100 ≥ 100 MPa), high flowability (slump flow ≥ 500 mm), and low shrinkage or micro expansion (autogenous shrinkage ≤ 100 με) were investigated. The following conclusions can be drawn:

Optimized CA incorporation (replacement ratios of 21.6% and 31.6%) effectively enhances the flowability and compressive strength of UHSC, while it provides limited autogenous shrinkage reduction and fails to meet the low shrinkage requirement.

The addition of steel fibers reduces the flowability of UHSC, especially for those with coarse aggregates. While the compressive strength of UHSC without coarse aggregates is monotonically enhanced by steel fibers, the compressive strength of UHSC with coarse aggregates exhibits an initial increase at 1% steel fibers and followed by a reduction at 2% steel fibers. Although steel fibers moderately reduce the autogenous shrinkage of UHSC, the minimum achieved autogenous shrinkage still exceeds the maximum requirement for core UHSC.

The incorporation of EA reduces the flowability and compressive strength of UHSC. Although the mixture incorporating 10% EA exhibits a significant autogenous shrinkage reduction (66.9%), it still fails to meet the low shrinkage requirement. Further increase in EA dosage would be impractical for maintaining adequate flowability and compressive strength.

The addition of SRA enhances the flowability but reduces the compressive strength of UHSC. Although 2% SRA achieves significant autogenous shrinkage reduction (51.7%), the value still exceeds the target threshold for low-shrinkage requirements.

Mixtures incorporating EA and SRA exhibit a superior autogenous shrinkage reduction effect compared to mixtures with only EA or SRA. Optimal performance is achieved through the combined use of coarse aggregates (21.6%) with hybrid admixtures (10% EA + 1~2% SRA), producing UHSC that fulfills all criteria for compressive strength, flowability, and debonding resistance.

Acknowledgments

This work is supported by the National Natural Science Foundation of China (Grant No. 52078136) and the National Key Laboratory of Materials for Major Infrastructure Engineering (EMMI2025203).

References

[1] Thai, S.; Thai, H. T.; Uy, B.; and Ngo, T. (2019) "Concrete-filled steel tubular columns: Test database, design and calibration," Journal of Constructional Steel Research, 157, pp. 161-181.

[2] Han, L. H.; Li, W.; and Bjorhovde, R. (2014) "Developments and advanced applications of concrete-filled steel tubular (CFST) structures: Members," Journal of Constructional Steel Research, 100, pp. 211-228.

[3] Li, L.; Lai, Z. C.; and Chen, B. C. (2024) "Ultra-high strength concrete filled steel tube members: Classification, experimental database, and design," Engineering Structures, 300, pp. 117210.

[4] Chen, B. C.; Li, L,; Luo, X.; Wei, J. G.; Lai, X. Y.; Liu, J. P.; Ding, Q. J.; and Li, C. (2020) "Review of ultra-high strength concrete filled steel tubes," Journal of Traffic and Transportation Engineering, 20(5), pp. 1-21.

[5] GB/T 31387-2015, (2015) "Reactive powder concrete," China national standardization administration (CNSAI) & General administration of quality supervision, inspection and quarantine of the People Republic of China (AQSIQ), Beijing, China.

[6] GB/T 50923-2013, (2013) "Technical code for concrete-filled steel tube arch bridges," Ministry of housing and urban-rural development of the People's Republic of China (MOHURD) & AQSIQ, Beijing, China.

[7] JTG/T D65-06-2015, (2015) "Specifications for design of highway concrete-filled steel tubular arch bridges," Ministry of Transport of the People's Republic of China, Beijing, China.

[8] Li, L., (2025) "Research on the ultimate bearing capactity of UHSC-filled steel tube columns

and arches [Dissertation]," University of Fuzhou University.

[9] Li, P. P.; Lu, Q. L.; Brouwers, and H. J. H. (2018) "Effect of coarse aggregates on the properties of ultra-high performance concrete (UHPC)," Construction and Building Materials, 170, pp. 649-659.

[10] Zeng, X. Z.; Deng, K. L.; Liang, H. W.; Xu, R. Y.; Zhao, C. H.; and Cui, B. (2020) "Uniaxial behavior and constitutive model of reinforcement confined coarse aggregate UHPC," Engineering Structures, 207, pp. 110261.

[11] Li, C.; Chen, B. C.; and Wei, J. G. (2019) "Shrinkage and mechanical properties of UHPC with coarse aggregate," Journal of Traffic and Transportation Engineering, 19(5), pp. 11-20.

[12] Miao, X. G.; Yuan, A. M.; Wang, K. Q.; Chen, Q.; Wang, X.; Kong, H.; Wang, J. Q. (2024) "Mechanical and autogenous shrinkage properties of coarse aggregate ultra-high performance concrete (CA-UHPC): The effect of mineral admixtures," Journal of Building Engineering,98, pp. 111154.

[13] Xue, J. Q.; Briseghella, B.; Huang, F. Y.; Nuti, C.; Tabatabai, H.; and Chen, B. C. (2020) "Review of ultra-high performance concrete and its application in bridge engineering," Construction and Building Materials, 260, pp. 119844.

[14] Jiao, Y,; Wang, J. Q.; Xu, Q. Z.; Qi, J. A.; Yao, Y. M. (2025) "Experimental study on early-age autogenous shrinkage and shrinkage induced stress of CA-UHPC under uniaxial restrained condition: Effects of coarse aggregate size and steel fiber volume fraction," Construction and Building Materials, 482, pp. 141236.

[15] Shen, P. L.; Lu, L. N.; He, Y. J.; Rao, M. J.; Fu, Z. D.; Wang, F. Z.; and Hu, S. G. (2018) "Experimental investigation on the autogenous shrinkage of steam cured ultra-high performance concrete,". Construction and Building Materials, 162, pp. 512-522.

[16] Chen, B. C.; Lin, Y. J.; Yang, J.; Huang, Q. W.; Huang, W.; and Yu, X. M. (2020) "Review on fiber function in ultra-high performance fiber reinfored concrete," Journal of Fuzhou University (Natural Science Edition), 48(1), pp. 58-68.

[17] Liu, L.; Chen, H.; He, Z.; Wang, P.; Cui, J. Y.; Cai, X. H.; and Sun, Y. Q. (2024) "Effect and mechanism of compound expansive agent on rheological, mechanical, and shrinkage properties of UHPC," Construction and Building Materials, 444, pp. 137730.

[18] Li, S. K.; Mo, L. W.; Deng, M.; and Cheng, S. K. (2021) "Mitigation on the autogenous shrinkage of ultra-high performance concrete via using MgO expansive agent," Construction and Building Materials, 312, pp. 125422.

[19] Shen, P. L.; Lu, L. N.; He, Y. J.; Wang, F. Z.; Lu, J. X.; Zheng, H. B.; and Hu, S. G. (2020) "Investigation on expansion effect of the expansive agents in ultra-high performance concrete," Cement and Concrete Composites, 105, pp. 103425.

[20] Park, J. J.; Yoo, D. Y.; Kim, S. W.; and Yoon, Y. S. (2012) "Combined influence of expansive and shrinkage reducing admixtures on the shrinkage behavior of ultra-high performance concrete," Key Engineering Materials, 488-489, pp. 242-245.

[21] Gong, J. Q.; Luo, H. K.; Zhang, Y.; Gong, X.; Xie, Z. L.; Wu, W. X.; and Dai, Y. F. (2021) "Effect of shrinkage reducing agent and HCSA expansion agent on mechanical properties and shrinkage properties of UHPC," Materials Report, 35(8), pp. 8042-8048+8063.

[22] Wei, J. G.; Luo, X.; Lai, Z. C.; and Varma, A. H. (2020) "Experimental behavior and design of high-strength circular concrete-filled steel tube short columns," Journal of Structural Engineering; 146(1), pp. 04019184.

[23] Funk, J. E.; and Dinger, D. R. (1994) "Predictive process control of crowded particulate suspensions," Kluwer Academic Publishers, Boston, the United States.

[24] Deng, Z. C.; Lian, Y. H.; and Zhao, L. Z. (2021) "Influence of expansion agent and shrinkage reducing agent on autogenous shrinkage of UHPC," Journal of Beijing University of technology, 47(1), pp. 61-68.

[25] GB/T 50080-2016, (2016) "Standard for test

method of performance on ordinary fresh concrete," MOHURD & AQSIQ, Beijing, China.

[26] GB/T 50082-2009, (2016) "Standard for test methods of long-term performance and durability of ordinary concrete," MOHURD & AQSIQ, Beijing, China.

[27] Snoeck, D.; Jensen, O. M.; and De Belie, N. (2015) "The influence of superabsorbent polymers on the autogenous shrinkage properties of cement pastes with supplementary cementitious materials," Cement and Concrete Research, 74, pp. 59-67.

[28] Li, P. P.; Yu, Q. L.; and Brouwers, H. J. H. (2017) "Effect of PCE-type superplasticizer on early-age behaviour of ultra-high performance concrete (UHPC)," Construction and Building Materials,153: 740-750.

[29] Xie, T.; Fang, C.; Mohamad Ali, M. S.; and Visintin, P. (2018) "Characterizations of autogenous and drying shrinkage of ultra-high performance concrete (UHPC): An experimental study," Cement and Concrete Composites, 91, pp. 156-173.

[30] Wu, F. H.; Xu, L. H.; Chi, Y.; Zeng, Y. Q.; Deng, F. Q.; and Chen, Q. (2020) "Compressive and flexural properties of ultra-high performance fiber-reinforced cementitious composite: The effect of coarse aggregate," Composite Structures, 236, pp. 111810.

[31] Xiong, M. X.; Liew, J. Y. R.; Wang, Y. B.; Xiong, D. X.; and Lai, B. L. (2020) "Effects of coarse aggregates on physical and mechanical properties of C170/185 ultra-high strength concrete and compressive behaviour of CFST columns," Construction and Building Materials, 240, pp. 117967.

[32] Lv. Y. J.; Zhang, W. H.; Wu, F.; Wu, P. P.; Zeng, W. Z.; and Wang, F. H. (2020) "Static mechanical properties and mechanism of C100 ultra-high performance concrete (UHPC) containing coarse aggregates," Science and Engineering of Composite Materials, 27(1), pp. 186-195.

[33] Shen, C.; Yang, D. S.; Lyu, Z. Q.; Yang, C. H.; and Yu, L. W. (2024) "Distribution of coarse aggregate and steel fibers in ultra-high performance concrete containing coarse aggregate (UHPC-CA) and their effect on the flexural performance," Construction and Building Materials, 421, pp. 135666.

[34] Gao, Z. Q.; Hu, J. T.; Yang, R. X.; Zhu, F. P.; Bai, P. X.; and Dong, L. (2024) "Micro-mechanical performance study of the interfacial transition zone in ultra-high performance concrete containing coarse aggregates based on digital image correlation method," Construction and Building Materials, 455, pp. 139162.

[35] Uysal, M. (2012) "The influence of coarse aggregate type on mechanical properties of fly ash additive self-compacting concrete," Construction and Building Materials, 37, pp. 533-540.

[36] Mishra, S.; and Mistry, R. (2020) "Reviewing some properties of ultra high performance concrete," International Journal of Engineering and Technology, 9(06), pp. 108-121.

[37] Wu, Z. M.; Shi, C. J.; He, W.; and Wu, L. M. (2016) "Effects of steel fiber content and shape on mechanical properties of ultra high performance concrete," Construction and Building Materials, 103, pp. 8-14.

[38] Yu, R.; Spiesz, P.; and Brouwers, H. J. H. (2014) "Mix design and properties assessment of ultra-high performance fibre reinforced concrete (UHPFRC)," Cement and Concrete Research, 56, pp. 29-39.

[39] Zhang, L. H.; Liu, J. P.; Zhou, H. X.; Liu, J. Z.; Zhang, Q. Q.; and Han, F. Y. (2017) "Effects of coarse aggregate and steel fiber on uniaxial tensile properties of ultra-high performance concrete," Materials Reports, 31(23), pp. 109-114.

[40] Liu, J. Z.; Han, F. Y.; Cui, G.; Zhang, Q. Q.; Lv, J.; Zhang, L. H.; and Yang, Z. Q. (2016) "Combined effect of coarse aggregate and fiber on tensile behavior of ultra-high performance concrete," Construction and Building Materials, 121, pp. 310-318.

[41] CECS 38-2004, (2004) "Technical specification for fiber reinforced concrete structures." China Planning Press, Beijing, China.

[42] Li, S. K.; Cheng, S. K.; Mo, L. W.; and Deng, M. (2020) "Effects of steel slag powder and expansive agent on the properties of ultra-high performance concrete(UHPC): Based on a Case Study," Buildings, 13, pp. 683.

[43] Fu, Z. D,; Lv, L. N.; Xiao, J.; He, Y. J.; and Shen, P. L. (2019) "Effect of calcium sulphoaluminate expansive admixture on properties of ultra-high performance concrete," Journal of Materials Science & Engineering, 37(4), pp. 559-564+594.

[44] Liu, C. J.; Zhang, X.; Cheng, S. K.; Li, S. K.; and Bao, M. (2024) "Mechanical properties, hydration behavior and shrinkage deformation of ultra-high performance concrete (UHPC) incorporating MgO expansive agent," Journal of Building Engineering, 96, pp. 110529.

[45] Chen, H.; Zhang, G. Z.; Ding, Q. J.; Yang, J.; Zhu, J. H.; and Qi, D. P. (2025) "Effect of expansive agent on lightweight micro-expansive ultra-high performance concrete: Properties, microstructure, and interfacial bonding in concrete-filled steel tube," Construction and Building Materials, 462, pp. 139996.

[46] Meddah, M. S.; Suzuki, M.; and Sato, R. (2011) "Influence of a combination of expansive and shrinkage-reducing admixture on autogenous deformation and self-stress of silica fume high-performance concrete," Construction and Building Materials, 25, pp. 239-250.

[47] Lee, K. H.; Nam, S. Y.; Min, S. E.; Lee, H. W.; Han, C.; and Ahn, J. W. (2016) "Characterizations of high early-strength type shrinkage reducing cement and calcium sulfo-aluminate by using industrial wastes," Journal of the Korean Ceramic Society, 53(2), pp. 215-221.

[48] Yoo, D. Y.; Chun, B.; and Kim, J. J. (2019) "Effect of calcium sulfoaluminate-based expansive agent on rate dependent pullout behavior of straight steel fiber embedded in UHPC," Cement and Concrete Research, 122, pp. 196-211.

[49] Huang, Z. Y.; Liu, Y. Q.; and Li, C. W. (2015) "Performance research of ultra high performance concrete incorporating HCSA expansion agent," Materials Reports, 29(2), pp. 116-121.

[50] Liu, L. M.; Fang, Z.; Huang, Z. Y.; Pei, B. Z.; and Wu, Y. Y. (2020) "Effects of expansive agent and super-absorbent polymer on performance of ultra-high performance concrete," Journal of the Chinese Ceramic Society, 48(11), pp. 1706-1715.

[51] Li, Y. B.; Deng, M. X.; Mo, L. W.; and Tang, M. S. (2012) "Strength and expansive stresses of concrete with MgO-type expansive agent under restrain conditions." Journal of Building Materials, 15(4), pp. 446-450.

[52] Yin, C. N.; Zong, W.; Wang, S. D.; Li, G. Q.; Li, Q. Y.; and Lu, L. C. (2011) "Effect of MgO on composition, structures and properties of Alite-calcium strontium sulphoalminate cement," Journal of the Chinese Ceramic Society, 39(1), pp. 20-24.

[53] Huang, C. B.; Zong, Z. J.; and Chen, P. Y. (2025) "Enhancing the performance of ultra-high performance concrete using expansive agent and pre-wetted biochar to produce a synergistic effect," Buildings, 15, pp. 1348.

[54] Tian, C. J,; Wang, Y. Z.; Du, Y. F.; Wang, Q.; and Yang, Q. L. (2024) "Synergistic effects of multiscale MgO expansion agent and SAP on the mechanical and shrinkage properties of UHPC," Journal of Materials in Civil Engineering, 36(3), pp. 4023610.

[55] Zhou, L.; Wang, Y. Z.; Zhang, G. N.; and Zhang, F. P. (2019) "Research progress in the effect of nano-MgO on the properties of cement-based materials," China Concrete and Cement Products, 5, pp. 13-18.

[56] Hu, S. G.; and Li, Y. (1999) "Research on the hydration, hardening mechanism, and microstructure of high performance expansive concrete," Cement and Concrete Research, 29, pp. 1013-1017.

[57] Guo, J. J; Zhang, S. W.; Qi, C. G.; Cheng, L.; and Yang, L. (2021) "Effect of calcium sulfoaluminate and MgO expansive agent on the mechanical strength and crack resistance of concrete," Construction and Building Materials, 299, pp. 123833.

[58] Aghaee, K.; Han, T. H.; Kumar, A.; and Khayat,

K. H. (2023) "Mechanism underlying effect of expansive agent and shrinkage reducing admixture on mechanical properties and fiber-matrix bonding of fiber-reinforced mortar," Cement and Concrete Research, 172, pp. 107247.

[59] Yoo, D. Y.; Kang, S. T.; Lee, J. H.; and Yoon, Y. S. (2013) "Effect of shrinkage reducing admixture on tensile and flexural behaviors of UHPFRC considering fiber distribution characteristics," Cement and Concrete Research, 54, pp. 180-190.

[60] Yoo, D. Y.; Kim, J.; Zi, G.; and Yoon, Y. S. (2015) "Effect of shrinkage-reducing admixture on biaxial flexural behavior of ultra-high-performance fiber-reinforced concrete," Construction and Building Materials, 89, pp. 67-75.

[61] Soliman, A. M.; and Nehdi, M. L. (2011) "Effect of drying conditions on autogenous shrinkage in ultra-high performance concrete at early-age," Materials and Structures, 44, pp. 879-899.

[62] Soliman, A. M.; and Nehdi, M. L. (2014) "Effects of shrinkage reducing admixture and wollastonite microfiber on early-age behavior of ultra-high performance concrete," Cement & Concrete Composites, 46, pp. 81-89.

[63] Teng, L.; Addai-Nimoh, A.; and Khayat, K. H. (2023) "Effect of lightweight sand and shrinkage reducing admixture on structural build-up and mechanical performance of UHPC," Journal of Building Engineering, 68, pp. 106144.

[64] Valipour, M.; and Khayat, K. H. (2018) "Coupled effect of shrinkage-mitigating admixtures and saturated lightweight sand on shrinkage of UHPC for overlay applications," Construction and Building Materials, 184, pp. 320-329.

[65] Yang, G.; Wu, Y. K.; Li, H.; Gao, N. X.; Jin, M.; and Hu, Z. L. (2021) "Effect of shrinkage-reducing polycarboxylate admixture on cracking behavior of ultra-high strength mortar," Cement and Concrete Composites, 122, pp. 104117.

[66] Zhang, W. Y.; Lin, H. X.; Xue, M. F.; Wang, S.; Ran, J. S.; Su, F. Q.; and Zhu, J. P. (2022) "Influence of shrinkage reducing admixtures on the performance of cementitious composites: A review," Construction and Building Materials, 325, pp. 126579.

[67] Zuo, W. Q.; Feng, P.; Zhong, P. H.; Tian, Q.; Gao, N. X.; Wang, Y. J.; Yu, C.; and Miao, C. W. (2017) Effects of novel polymer-type shrinkage-reducing admixture on early age autogenous deformation of cement pastes," Cement and Concrete Research, 100, pp. 413-422.

[68] Wang, T. Y.; Gong, J. Q.; Chen, B.; Gong, X.; Luo, H. K.; Zhang, Y.; and Qu, Z. G. (2021) Effects of shrinkage reducing agent and expanded cement on UHPC fluidity, mechanical properties, and shrinkage performance," Advances in Materials Science and Engineering, 2021, pp. 9045754.

[69] Yuan, T. F.; Kim, S. K.; Koh, K. T.; and Yoon, Y. S. (2018) "Synergistic benefits of using expansive and shrinkage reducing admixture on high-performance concrete," Materials, 11, pp. 2514.

[70] Corinaldesi, V. (2012) "Combined effect of expansive, shrinkage reducing and hydrophobic admixtures for durable self compacting concrete," Construction and Building Materials, 36, pp. 758-764.

[71] Collepardi, M.; Borsoi, A.; Collepardi, S.; Olagot, J. J. O.; and Troli, R. (2005) "Effects of shrinkage reducing admixture in shrinkage compensating concrete under non-wet curing conditions," Cement and Concrete Composites, 27, pp. 704-708.

[72] Wang, C.; Yang, C. H.; Liu, F.; Wan, C. J.; and Pu, X. C. (2012) "Preparation of ultra-high performance concrete with common technology and materials," Cement & Concrete Composites, 34, pp. 538-544.

[73] Pu, X. C.; Yan, W. N.; and Wang, C. (1998) "Preparation technology of 100~150MPa ultra-high strength and high performance concrete," China Concrete and Cement Products, 6, pp. 3-7.

[74] Peng, Y.; Gao, Y. X.; Wu, X.; Cheng, J. B.; Lin, J. C.; Jiang, J. N.; and Jia, L. L. (2015) "Influence of coarse aggregate on the performance of C140 concrete," China Concrete and Cement

Products, 1,pp. 15-18.

[75] Miao, X. G.; Yuan, A. M.; Wang, K. Q.; Chen, Q.; Wang, Q.; Wang, X.; Kong, H.; and Wang, J. Q. (2024) "Mechanical and autogenous shrinkage properties of coarse aggregate ultra-high performance concrete (CA-UHPC): The effect of mineral admixtures," Journal of Building Engineering, 98, pp. 111154.

[76] Xu, L. H.; Wu, F. H.; Chi, Y.; Cheng, P.; Zeng, Y. Q.; and Chen, Q. (2019) "Effects of coarse aggregate and steel fibre contents on mechanical properties of high performance concrete," Construction and Building Materials, 206, pp. 97-110.

[77] Hassan, A. M. T.; Jones, S. W.; and Mahmud, G. H. (2012) "Experimental test methods to determine the uniaxial tensile and compressive behaviour of ultra high performance fibre reinforced concrete (UHPFRC),"Construction and Building Materials, 37, pp. 874-882.

[78] Senapathi, A.; and Peiris, A. (2025) "A comprehensive study of steel fiber alternatives on mechanical properties, long-term performance, and durability of ultra-high-performance concrete: A review," Journal of Building Engineering, 108, pp. 112900.

[79] Hannawi, K.; and Bian, H. (2016) "Prince-Agbodjan W, Raghavan B. Effect of different types of fibers on the microstructure and the mechanical behavior of ultra-high performance fiber-reinforced concretes," Composites Part B: Engineering, 86, pp. 214-220.

[80] Zhang, R. X.; and Panesar, D. K. (2017) "New approach to calculate water film thickness and the correlation to the rheology of mortar and concrete containing reactive MgO," Construction and Building Materials, 150, pp. 892-902.

[81] Cao, F. Z.; Miao, M.; and Yuan, P. Y. (2018) "Effects of reactivity of MgO expansive agent on its performance in cement-based materials and an improvement of the evaluating method of MEA reactivity," Construction and Building Materials, 187, pp. 257-266.

[82] Du, J.; Tan, X.; Wang, Y. H.; Bao, Y.; and Meng, W. N. (2024) "Reducing the cracking potential of ultra-high-performance concrete (UHPC) with the prewet expansive agent," Construction and Building Materials, 431, pp. 136597.

[83] Guo, Q. C.; Wang, Z.; Dang, Y. D.; Qian, J. S.; and Jiang, N. (2014) "Investigation on compatibility of Polycarboxylic Superplasticzer and shrinkage reducing agent," Journal of Building Materials, 17(2), pp. 239-245.

[84] Wang, T. Y.; Gong, J. Q.; Chen, B.; Gong, X.; Luo, H. K.; Zhang, Y.; and Qu, Z. G. (2021) "Effects of shrinkage reducing agent and expanded cement on UHPC fluidity, mechanical properties, and shrinkage performance," Advances in Materials Science and Engineering, 2021, pp. 9045754.

[85] Liu, J. H.; Farzadnia, N.; Shi, C. J.; Ma, X. W. (2019) "Shrinkage and strength development of UHSC incorporating a hybrid systemof SAP and SRA," Cement and Concrete Composites, 97, pp. 175-189.

[86] Alsalman, A.; Dang, C. N.; Prinz, G. S.; and Micah Hale, W. (2017) "Evaluation of modulus of elasticity of ultra-high performance concrete," Construction and Building Materials, 153, pp. 918-928.

[87] Sun, W.; Chen, H. S.; Luo, X.; and Qian, H. P. (2001) "The effect of hybrid fibers and expansive agent on the shrinkage and permeability of high-performance concrete," Cement and Concrete Research, 31(4), pp. 595-601.